https://doi.org/10.1016/j.biortech.2021.125555

Impacts of Different Activation Process on the Carbon Stability of Biochar for Oxidation Resistance

Zibo Xu [a], Mingjing He [a], Xiaoyun Xu [b], Xinde Cao [b], Daniel C.W. Tsang [a,*]

[a] Department of Civil and Environmental Engineering, The Hong Kong Polytechnic University, Hung Hom, Kowloon, Hong Kong, China

[b] School of Environmental Science and Engineering, Shanghai Jiao Tong University, Shanghai 200240, China

*Corresponding author email: dan.tsang@polyu.edu.hk

Abstract:

Biochar activation is widely used to improve its capability for environmental application, while its impact on carbon sequestration potential is still unknown. Herein, the oxidation-resistance stability of biochar with different activation processes was first evaluated, which is crucial for the sustainable production of activated biochar. Thermal activation enhanced the thermal stability of biochar with a higher R_{50} as 61.5−62.7%, whereas a higher carbon loss of 15.2−17.2% after chemical oxidation was found. Physical activation of biochar failed to affect thermal stability, but it still weakened its chemical stability. By contrast, chemical activation with H_2SO_4 improved the stability for both chemical- (6.7% carbon loss) and thermal-oxidation (R_{50} as 66.2%). Further analysis revealed that the thermal stability of activated biochar was controlled by aromaticity, while the surface area was a vital factor for the chemical stability. Our findings could serve as a reference to mediate the trade-offs between biochar stability and other application.

Keywords: Activated biochar; Carbon sequestration; Carbon stability; Oxidation resistance.

1. Introduction

Biochar, a carbon-rich by-product from the biomass pyrolysis process, attracts great interest as a valuable tool for carbon abatement in the last decade (Cross & Sohi, 2013; Han et al., 2020). As a carbon-negative material, biochar production and application could effectively reduce the total carbon emission (Lehmann, 2007; Leng & Huang, 2018; Leng et al., 2019). Moreover, various environmental applications (*e.g.,* water pollution control) can also be realized by biochar in the meantime (Ahmad et al., 2014; Li et al., 2017; Shaheen et al., 2019), which improves the value of biochar utilization with a win-win effect for the environment.

Although several studies find that the pristine biochar can effectively achieve water and wastewater remediation, including toxic metals immobilization (Cao & Harris, 2010; Shaheen et al., 2019) and organic pollutants removal (Liang et al., 2019), its capacity is restricted by the low surface reactivity of the un-activated biochar (*e.g.,* surface area and surface functionality) (Cheng et al., 2017; Zhang et al., 2020). To improve the performance of biochar for environmental remediation, various activation methods are conducted for a higher surface reactivity (Ahmed et al., 2016; Cheng et al., 2017; Sajjadi et al., 2019). Physical activation (*e.g.,* steam activation and CO_2 activation), chemical activation such as acid pre-treatment, and thermal activation were widely used for biochar because of their convenience and remarkable improvement on biochar activity (Cheng et al., 2017).

Different activation processes principally cause varying properties of biochar

(Kazemi Shariat Panahi et al., 2020; Zhou et al., 2021). For physical activation, active carbon atoms could be removed by the insert steam or CO_2 during high-temperature pyrolysis (**Eq.1**−**2**) and led to an increased porosity and surface area (Sajjadi et al., 2019). For example, a significantly higher surface area of activated biochar was found after steam activation at both 300 °C and 550 °C compared with the pristine biochar (189.2−397.1 $m^2\ g^{-1}$ > ~1 $m^2\ g^{-1}$) (Lou et al., 2016). Meanwhile, the formed reducing gas might further react with the carbon surface, contributing to different surface chemistry (*i.e.,* surface O-moiety) on biochar (**Eq.3**−**4**) (Anto et al., 2021; Kim et al., 2021). Different from physical activation, chemical activation is usually conducted before or after the pyrolysis process by mixing feedstocks or biochar with the active agent. Acid activation with inorganic acids like H_2SO_4 and HNO_3 was widely used to improve the surface area and O-moieties of biochar (Hadjittofi et al., 2014; Iriarte-Velasco et al., 2016). Moreover, using a high temperature (>800 °C) to thermal-activate the biochar with the formation of graphitic and turbostratic char is also reported in recent years (Sajjadi et al., 2019; Xiao et al., 2018; Ghodake et al., 2021). This kind of biochar naturally contained a higher surface area with rich carbon defects, and it was widely used for catalytic and electrochemical reactions (Huggins et al., 2015; Wan et al., 2019; Xiao & Chen, 2017).

$$H_2O\ (g) + C \rightarrow H_2 + CO \qquad \text{Eq.1}$$

$$C + CO_2 \rightarrow 2CO \qquad \text{Eq.2}$$

$$H_2 + \equiv C{-}O \rightarrow C + H_2O \qquad \text{Eq.3}$$

$$CO + \equiv C{-}O \rightarrow C + CO_2 \quad \text{Eq.4}$$

With the booming studies about biochar activation, a new question about the carbon stability of these activated biochars emerged. Since all activation methods target the improvement of the biochar's surface reactivity, the carbon sequestration potential of biochar could be affected. The higher surface area of activated biochar might result in an increased chance of reacting with the oxidizing moiety (*e.g.,* O_2) in the environment, which would probably decrease the long-term carbon sequestration potential of biochar (Wang et al., 2020). Change of surface functionality and carbon structure would also directly affect the stability of biochar (Kim et al., 2021; Leng & Huang, 2018; Spokas, 2010). Since long-term carbon stability is the major concern for the sustainable production and application of biochar, the trade-off between carbon stability and biochar surface reactivity should be considered before selecting proper activation methods. Different activation methods might produce the activated biochar with distinct properties and thus led to different carbon stability. However, the current study about biochar activation mainly focused on the surface reactivity instead of the properties related to carbon stability. The change of the carbon sequestration potential of biochar during different activation processes was still unknown, and understanding the impact of activation on biochar stability was vital for the sustainable production of biochar.

We hypothesize that the activation process would significantly affect the carbon stability of the biochar for oxidation resistance. To test this hypothesis, we conducted this study to (1) evaluate the stability of biochar produced from different activation

methods and (2) identify the decisive factor of activated biochar for carbon stability. Biochars with different pyrolysis temperatures from 450−950 °C and various activation methods (steam activation, CO_2 activation, and acid activation) were prepared in this study. Besides, the stability of activated biochar was evaluated by determining basic properties and the "oxidation resistance" property. Two oxidation methods, including chemical oxidation by a strong oxidant (*i.e.,* $K_2Cr_2O_7$) and thermal oxidation by heating under air environment through Thermogravimetric Analysis (TG) (Leng et al., 2019; Yang et al., 2018; Yang et al., 2016), were used to test the stability of activated biochar. Overall, this study evaluates the impact of different activation methods on the stability of biochar, guiding the production, activation, and selection of biochar in the future.

2. Materials and Methods

2.1 Chemicals and Raw Materials

Local light yard waste (LYW), collected from EcoPark in Hong Kong, was selected as the raw biomass for this study. The biomass was dried at 60 °C in the oven for 24 h before pyrolysis. All chemicals used in this study were of analytical grade.

2.2 Preparation of Biochar and Biochar Activation

The biochar used in this study was produced from LYW through slow pyrolysis under N_2-atmosphere at target temperature with a heating rate of 10 °C min^{-1} and a holding time of 60 min. Six temperatures as 450, 550, 650, 750, 850, and 950 °C were used for the biochar preparation, and the resultant biochars were named BC-X, where

X indicates the pyrolysis temperature. Higher pyrolysis temperatures (850 and 950 °C) could be considered as the thermal-activation methods for biochar (Sajjadi et al., 2019), while the other pyrolysis temperature mainly acted as the control.

Moreover, two physical activation and one chemical activation methods were used for biochar activation. For steam activation, N_2 gas was used as the purging gas for LYW pyrolysis to the target activated temperature (650, 750, and 850 °C) with a heating rate of 10 °C min^{-1}. The steam feeding pump started 10 min before reaching the target pyrolysis temperature, and then the steam would touch the heating zone with biochar. This activation process will keep for 60 min, and the resultant biochar will be named BCX-S, where X indicates the activation temperature. CO_2 activation was achieved by using CO_2 as the purging gas for the pyrolysis directly. The highest temperature was set as 650, 750, and 850 °C for LYW pyrolysis with the same heating rate and holding time (10 °C min^{-1} and 60 min). These activated biochars were denoted as BC650-C, BC750-C, and BC850-C, respectively. Acid activation was realized by treating the LYW with 1 M H_2SO_4 (solid to liquid ratio as 1:20) for 24 h. The acid-treated LYW was filtered and dried at 60 °C for 24 h before pyrolysis. Only 750 °C was chosen as the pyrolysis temperature (BC750-A), and the heating settings were the same as the other activation process (10 °C min^{-1} and 60 min). All biochars were crushed to pass a 120-mesh sieve and stored in a dry container before further usage.

2.3 Biochar characterization

The surface area of different biochar was determined by N_2 adsorption-desorption

123 isotherms obtained from a surface area analyzer at 77 K (BET, Quantachrome Autosorb,
124 USA). The ultimate elemental analysis (EA, Vario EL cube, Germany) was used to
125 estimate the CHONS content in the biochar samples. The atomic ratio of H/C and O/C
126 was calculated to identify the properties of biochar. Moreover, the aromatic index (AI),
127 representing the aromaticity of biochar, was also calculated based on **Eq.5**.

128 $$\mathrm{AI} = \frac{1+[C]-[O]-0.5[H]}{[C]-[O]-[N]} \quad \textbf{Eq.5}$$

129 The X-ray photoelectron spectroscopy (XPS, Thermo Scientific Nexsa) with Al Kα
130 radiation was used to investigate the composition and chemical state of the elements on
131 the sample surfaces. The binding energy of all characteristic peaks was calibrated with
132 carbon C1s core level at 284.8 eV, and the component peaks were identified by
133 comparing their binding energies with the literature values (Xu et al., 2020; Yang et al.,
134 2016). To evaluate the surface functionality of biochar, the ratio of the O-moiety (sum
135 of –C–O, –C=O, and –COO) to –C=C was calculated.

136 2.4 Stability of biochar for thermal-oxidation resistance

137 The stability of biochar for thermal-oxidation resistance was evaluated by the TG
138 analysis under the air environment (Leng et al., 2019; Yang et al., 2016). Weight loss
139 associated with the thermal oxidation of all these biochars was detected in an air
140 environment using thermogravimetry/derivative thermogravimetry (TG/DTG). The
141 thermal analysis started at 30 °C with a ramping rate of 10 °C min^{-1} to 1000 °C. An
142 indicator (R50) was used to evaluate the oxidation recalcitrance of biochar during TG
143 analysis (**Eq.6**) with graphite as the reference.

$$R_{50,biochar} = \frac{T_{50\ biochar}}{T_{50\ graphite}} \times 100\% \quad \textbf{Eq.6}$$

$T_{50\ biochar}$ and $T_{50\ graphite}$ are the temperature values corresponding to 50% weight loss by oxidation of biochar and graphite, respectively.

2.5 Stability of biochar for chemical-oxidation resistance

The stability of biochar for chemical-oxidation resistance was identified by $K_2Cr_2O_7$ oxidation methods (Leng et al., 2019; Nan et al., 2020; Yang et al., 2018). About 0.1g biochar was added into a glass test tube with 40 mL of 0.1 M $K_2Cr_2O_7$/2 M H_2SO_4 solution. Chemical oxidation would be conducted at 55 °C for 60 h in triplicates. The carbon loss amount was determined by the transition of Cr(VI) concentration according to **Eq.7,** and the carbon loss proportion was calculated based on the carbon content in biochar as detected by EA. The Cr(VI) concentration was detected by the diphenyl-carbazide spectrophotometric method at 540 nm (Dong et al., 2011; Xu et al., 2020).

$$2K_2Cr_2O_7 + 3C + 8H_2SO_4 \rightarrow 2K_2SO_4 + 2Cr_2(SO_4)_3 + 3CO_2\uparrow + 8H_2O \quad \textbf{Eq.7}$$

2.6 Pearson Correlation Coefficient Analysis

The relationship between carbon stability for oxidation resistance and the basic properties of biochar was evaluated byPearson Correlation Coefficient (PCC) analysis. R_{50} and carbon loss by Cr(VI) oxidation were selected as the stability index to represent the thermal-oxidation resistance and chemical-oxidation resistance, respectively. Basic properties of biochar, including aromaticity (*i.e.,* H/C ratio and AI), O-moiety content (*i.e.,* O/C ratio and O-moiety obtained from XPS analysis), carbon proportion from TG

165 analysis, and surface area, were all involved during the relationship analysis.

166

167 **3. Results and Discussions**

168 3.1 O-moieties of activated biochars

169 O/C ratio obtained from EA was first adopted to reveal the change of functionality
170 of activated biochar (**Figure 1a**, **Figure 1b**, and **Table 1**). An apparent decrease of the
171 O/C ratio from 0.24 to 0.07 was found with the pyrolysis temperature from 450 °C to
172 750 °C, and it kept constant as 0.07−0.09 under the followed increasing temperature
173 (750−950 °C). Increasing temperature from 450 °C to 750 °C could induce the decrease
174 of O-moiety (Manyà et al., 2014; Xu et al., 2020), while no further change of O-moiety
175 was found under extremely high pyrolysis temperature (850−950 °C) for thermal
176 activation. Similar results were found by the O-moiety content detected by XPS
177 analysis (**Figure 1a** and **Table 2**). No noticeable alternation about the surface functional
178 group could be found under the high pyrolysis temperature over 750 °C, further
179 indicating the limited impact of thermal activation on biochar's functionality compared
180 with the biochar produced with regular high temperature (*i.e.,* BC750).

181 Unlike the thermal activation, a noticeable change of the O/C ratio was found with
182 steam and CO_2 activation (**Figure 1b**). Physical activation at relatively low
183 temperatures (*i.e.,* 650 °C and 750 °C) increased the O/C ratio of the biochar, whereas
184 a slight decrease from 0.09 to 0.05−0.07 was found at 850 °C. Contrasting change of
185 the O/C ratio implied the different reactions between the low and high pyrolysis

temperatures. At low pyrolysis temperature, the introduction of the O atom from H_2O and CO_2 into the carbon surface might be dominant (**Eq.8**−**9**) (Sajjadi et al., 2019), which resulted in the increase of O-moiety on biochar. An increase of phenolic groups, carboxylic groups, and the O/C ratio of biochar after the physical activation process was also found by related research (Feng et al., 2017; Kwak et al., 2019) due to the oxidizing capacity of steam and CO_2. However, at the high activated temperature (*i.e.,* 850 °C), the reducing reaction among the gas and carbon surface became the primary reaction, which led to the decline of O content (**Eq.3**−**4**) (Sajjadi et al., 2019). A decrease of the O-content after activation at a high temperature (> 700 °C) was also found by both Sun et al. (2020) and Yek et al. (2020) due to the reduction reaction with the biochar surface. It is worth noting that a higher O/C ratio was found after steam activation compared with CO_2 activation at the same activated temperature due to the stronger reactivity of the steam (Liu et al., 2020b).

$$H_2O + C \rightarrow \equiv C{-}O + H_2 \qquad \textbf{Eq.8}$$

$$C + CO_2 \rightarrow CO + \equiv C{-}O \qquad \textbf{Eq.9}$$

Interestingly, physical activation induced a high O-moiety on the surface of biochar at all three activated temperatures based on XPS analysis (**Figure 1b**), which is different from the EA results. The higher O-moiety/−C=C ratio as 0.17 after steam activation and 0.16−0.18 after CO_2 activation was found compared with the pristine biochar (0.15). Since XPS analysis normally provides information about the surface of the biochar (~3−5 nm), the high O-moiety detected by XPS evidenced the remarkable surface

reactivity of the activated biochar.

Chemical activation by H_2SO_4 also showed a noticeable impact on the O-moiety on biochar that caused a higher O/C ratio (0.13) on BC750-A than the origin biochar and physically activated biochar (BC750, BC750-S, and BC750-C, 0.07−0.11) (**Figure 1b** and **Table 1**) due to the oxidation capacity of H_2SO_4 (Lau et al., 2017). However, the surface O-moiety content (O-moiety/−C=C ratio as 0.15) was similar to BC750 (0.15). Lower surface O-moiety content of acid-modified biochar (BC750-A) compared with other modification methods (BC750-C and BC750-S) might be attributed to the surface coverage with sulfate mineral and organic compounds, which was also found in the relevant study (Chen et al., 2021; Liu et al., 2020a).

This different O/C ratio and surface O-moiety might contribute to the distinct stability of the activated biochar. According to Spokas (2010), the lower O/C ratio represented higher carbon stability of biochar, and the biochar with an O/C ratio lower than 0.2 was perceived as the most stable, possessing an estimated half-life over ~1000 years. Based on this, activation under 650−750 °C might lead to lower stability on the produced activated biochar, especially for the physically activated biochar at 650 °C (O/C ratio as 0.25 for BC650-S and 0.20 for BC650-C).

3.2 Aromaticity of activated biochar

The aromaticity of biochar is also a critical indicator of its stability. H/C atomic ratio and Aromatic Index (AI) were calculated based on the element content (**Eq.5**) to evaluate the transition of the aromaticity during the activation process. As shown in

228 **Figure 1c** and **Table 1**, higher pyrolysis temperature over 850 °C resulted in a lower
229 H/C ratio (0.10) and higher AI (1.10), both evidencing the increase of the aromaticity
230 with thermal activation (Xiao et al., 2018). Higher pyrolysis temperature, especially
231 over 700 °C (percolation temperature), will lead to the expansion of graphene regions
232 and aromatic clusters and thus formed biochar with high aromaticity (Manyà et al.,
233 2014; Pignatello et al., 2017; Xu et al., 2020).

234 Similarly, physical and chemical activation also induced an increase in the
235 aromaticity of the biochar. A relatively lower H/C as 0.05−0.15 was detected on the
236 activated biochar compare with the pristine biochar (0.10−0.29) (**Figure 1d**).
237 Meanwhile, AI also slightly raised from 1.00−1.10 to 1.10−1.15 after the activation
238 process (**Figure 1d**). A similar decrease of the H/C ratio from 0.23−0.26 to 0.14−0.17
239 with the increase of aromaticity was also found by Kwak et al. (2019) after steam
240 activation for biochar at 700 °C. Higher aromaticity usually represented a stable carbon
241 structure in the biochar (Han et al., 2018). Therefore, results from the H/C ratio and AI
242 indicated that the activation process would enhance the stability of the biochar, which
243 contrasts with the results from the O/C ratio. To further identify the stability of biochar
244 for oxidation resistance, thermal oxidation and chemical oxidation methods were both
245 conducted in the following section.

246 3.3 Thermal-oxidation resistance

247 Thermal oxidation was conducted by TG analysis under air environment (Harvey
248 et al., 2012), and the results were shown in **Figure 2** and **Appendix**. It could be found

249 that weight loss of all activated biochar mainly happened around 400 °C and finished
250 at ~600 °C (**Figure 2a**, **Figure 2b**, and **Appendix**). R_{50} of each biochar was calculated
251 with the reference of graphite (**Eq.6**), and the results were shown in **Figure 2c** and
252 **Figure 2d**. It could be found that thermally activated biochar (BC850 and BC950)
253 obtained a higher R_{50} as 61.5−62.7% compared with the low-temperature produce
254 biochar (53.3−58.2%), and the R_{50} index of low-temperature produced biochar (<
255 750 °C) was similar to the thermal stability of biochar in the relevant study (56.2−60.5%)
256 (Liu et al., 2020c). However, no remarkable change of the R_{50} was found after steam
257 activation and CO_2 activation compared with the pristine biochar (**Figure 2d**). A similar
258 R_{50} as 56.3−57.2 %, 58.8−58.9 %, and 60.8−62.1% was shown for 650, 750, and 850 °C
259 activated biochar, respectively. Interestingly, chemical activation by H_2SO_4 gave an
260 apparent high R_{50} of 66.2% on the BC750-A, which might be attributed to the change
261 of minerals composition in biochar during the acid treatment (Liu et al., 2020c; Nan et
262 al., 2021). These results indicated that different activation methods offered distinct
263 stability for thermal oxidation resistance. It is worth noting that a high R_{50} could also
264 represent a lower carbon mineralization rate during the abiotic and biotic incubation
265 (Harvey et al., 2012).

266 Based on the TG analysis, carbon speciation could be divided into the following
267 species with different stability (**Figure 3** and **Appendix**) (Leng et al., 2019; Leng et al.,
268 2018): volatile organic C (degradation range of 30–200 °C), labile organic-C (cellulose,
269 aliphatic-C, and carbohydrates with a degradation range of 200–380 °C), recalcitrant

organic-C (lignin and aromatic C with a degradation range of 380–475 °C), refractory organic-C (poly-condensed forms of lipids and aromatic-C with a degradation range of 475–600 °C), and inorganic-C (elemental-C and carbonate with a degradation range of 600–1000 °C). As shown in **Figure 3a**, refractory organic C was the main form of the carbon in biochar after thermal activation (73.0% for BC850 and 72.0% for BC950), representing higher stability than low-temperature produced biochar which contained a lower proportion of refractory organic-C (25.8–60.5%). However, physical activation failed to change the speciation of carbon in all three activated temperatures (**Figure 3b**), evidencing the marginal change of the stability of the physically activated biochar for the thermal-oxidation resistance. A higher stable carbon fraction (refractory organic C) as 85.9% was also found after chemical activation with H_2SO_4, further supporting the higher thermal stability of BC750-A from the high R_{50}.

In short, for the thermal-oxidation resistance, thermal activation with high pyrolysis temperature and chemical activation by H_2SO_4 could strengthen the carbon stability of biochar, while limited change was found after physical activation by both steam and CO_2.

3.4 Chemical-oxidation resistance

$K_2Cr_2O_7$ (Cr(VI)) with H_2SO_4 was used to oxidize different activated biochar chemically, and the carbon loss proportion was calculated to evaluate the carbon stability for chemical-oxidation resistance (**Figure 4**). Surprisingly, we found that biochar produced with high pyrolysis temperature had a relatively higher carbon loss

(15.2% for BC850 and 17.2% for BC950) during the Cr(VI) oxidation compared with low-temperature biochar (2.6−12.7%) (**Figure 4a**). This result was different from the previous studies that higher pyrolysis temperature usually caused higher stability for the chemical-oxidation resistance (Han et al., 2018; Liu et al., 2020d; Nan et al., 2021). The possible reason was that previous studies mainly focused on the biochar produced lower than 700 °C, while the turning point in this study was within 650−750 °C. 700 °C could be a crucial temperature for biochar production and activation due to the appearance of graphene regions in biochar over this temperature (Pignatello et al., 2017), thus providing a relatively higher reactivity and lower chemical-oxidation resistance of the produced biochar (Xu et al. 2020). Similar to the thermal activation, physical activation also alleviated the carbon stability of biochar for Cr(VI) oxidation. Carbon loss increased from 2.6% to 5.8−6.7%, from 9.3% to 10.1−13.4%, and from 15.2% to 17.3−22.8% for activated temperature as 650, 750, and 850 °C, respectively (**Figure 4b**). Steam-activated biochar had lower stability with a higher carbon loss than CO_2-activated biochar due to the higher O-functionality **(Figure 1b**) caused by the strong reactivity of steam (Liu et al., 2020b). The impact of physical and thermal activation on the chemical-oxidation resistance was different compared with thermal-oxidation resistance, which indicated a different decisive factor on the stability. By contrast, chemical activation by H_2SO_4 still enhanced the carbon stability for chemical-oxidation resistance, which decreased the carbon loss proportion from 9.3% (BC750) to 6.7% (BC750-A) (**Figure 4b**). Lower surface O-moiety content (**Figure 1b**) on the

surface of BC750-A might contribute to the higher stability since the O-moiety might be the main reaction site for oxidants (*i.e.,* Cr(VI)) (Xu et al., 2020). The increased stability of BC750-A for chemical-oxidation resistance was similar to the thermal-oxidation resistance.

Consequently, thermal and physical activation decreased the biochars' stability for chemical-oxidation resistance, which was different from thermal-oxidation resistance. Meanwhile, chemical activation with H_2SO_4 still increased the carbon stability of biochar for chemical-oxidation resistance, similar to its impact on thermal-oxidation resistance. These results implied the inconsistent influence mechanisms and decisive factor of activated biochars' stability for chemical and thermal oxidation resistance.

3.5 The decisive factor for activated biochars' stability

To evaluate the decisive factor of activated biochar for thermal-oxidation resistance and chemical-oxidation resistance, Pearson correlation coefficient (PCC) analysis between the carbon stability index and different basic properties was conducted (**Appendix** and **Figure 5**). R_{50} (**Figure 2**) and carbon loss by Cr(VI) oxidation (**Figure 4**) were selected as the index to represent the stability for thermal-oxidation resistance and chemical-oxidation resistance, respectively. Basic properties of biochar including aromaticity (*i.e.,* H/C ratio and AI, **Figure 1**), O-moiety content (*i.e.,* O/C ratio and O-moiety obtained from XPS analysis, **Figure 1**), carbon proportion from TG analysis (**Figure 3**), and specific surface area (SSA, **Appendix**) were all involved.

Based on the PCC analysis, no relationship could be found between chemical

stability and thermal stability (PCC as 0.41 $p>0.05$), further indicating the distinct decisive factor between them. The R_{50} of different biochar was positively related ($p < 0.01$) to refractory organic-C (0.98) or inorganic-C (0.84), whereas a negative relationship ($p < 0.01$) was also found with labile organic-C (-0.71) or H/C ratio (-0.78). This result confirmed that aromatic carbon in the forms of refractory organic-C or inorganic-C with higher thermal stability determined the activated biochar's stability for thermal-oxidation resistance (Leng & Huang, 2018). More aromatic carbon in the activated biochar offered higher stability during thermal oxidation. However, no significant relationship could be found between the C loss proportion by Cr(VI) oxidation and surface O-moiety or aromaticity of activated biochar (**Figure 5**). The only related factor was the surface area of the activated biochar (0.77, $p < 0.01$). This result was inconsistent with the previous studies that the chemical oxidation stability of biochar was negatively related to the O/C or H/C ratio (Chen et al., 2016; Han et al., 2018; Liu et al., 2020c). The possible reason might be that the biochar used in the previous studies was produced within 300−700 °C without activation (Chen et al., 2016; Han et al., 2018). These biochars normally had a similar and low surface area compared with the activated biochar, and thus the O/C and H/C ratio become the dominant factors. It could be speculated that the higher specific surface area of activated biochar facilitated the chemical oxidation process with oxidants and thus led to lower stability for the chemical-oxidation resistance. The enhanced reactivity from the increased surface area of activated biochar might be one decisive factor for the stability of

chemical-oxidation resistance when high pyrolysis temperature is applied.

3.6 Future research perspective

Our study revealed that different activation methods would affect the carbon sequestration potential of the produced biochar, which could serve as a critical reference for the production of activated biochar as a sustainable and carbon-negative material. However, future research based on the following issues and challenges was still needed to accelerate the broad production and application of the activated biochar: (i) Techno-economic prospects of activated biochar production considering feedstocks, the conversion and activation technology, activation agent, energy input/output, and the inclusion of carbon sequestration subsidies or carbon credits reflecting the value of greenhouse gas mitigation; (ii) Long-term carbon stability and sequestration potential of different activated biochar under practical application scenario; (iii) Trade-off between reactivity and carbon stability of activated biochar based on an overall concern about the economic, environmental, and social aspects; (iv) carbon footprint of the activated biochar application considering production process, activation process, and the carbon loss of the activated biochar during the application.

4. Conclusions

The impacts of different activation processes on the carbon stability of biochar were described in this study. Both thermal activation and physical activation weaken biochar's stability for chemical-oxidation resistance, while only the thermal activation

enhanced the stability for thermal-oxidation resistance. By contrast, chemical activation with H_2SO_4 improved the stability for both chemical and thermal oxidation. Further analysis revealed the aromaticity controlled the thermal stability of activated biochar, while the surface area was a vital factor to compromise the chemical-oxidation resistance. This study could guide biochar production and activation to balance carbon sequestration and other environmental applications.

Appendix

E-supplementary data for this work can be found in the e-version of this paper online.

Acknowledgments

We appreciate the financial support from the Hong Kong Research Grants Council (PolyU 15222020) and Hong Kong Environment and Conservation Fund (ECF Project 87/2017) for this study. We also acknowledge the equipment support provided by the University Research Facility in Materials Characterization and Device Fabrication (UMF) of the Hong Kong Polytechnic University

391 **Reference**

392 1. Ahmad, M., Rajapaksha, A.U., Lim, J.E., Zhang, M., Bolan, N., Mohan, D.,
393 Vithanage, M., Lee, S.S., Ok, Y.S. 2014. Biochar as a sorbent for contaminant
394 management in soil and water: A review. *Chemosphere*, **99**, 19-33.
395 2. Ahmed, M.B., Zhou, J.L., Ngo, H.H., Guo, W., Chen, M. 2016. Progress in the
396 preparation and application of modified biochar for improved contaminant removal
397 from water and wastewater. *Bioresource Technology*, **214**, 836-851.
398 3. Anto, S., Sudhakar, M.P., Shan Ahamed, T., Samuel, M.S., Mathimani, T.,
399 Brindhadevi, K., Pugazhendhi, A. 2021. Activation strategies for biochar to use as an
400 efficient catalyst in various applications. *Fuel*, **285**, 119205.
401 4. Cao, X., Harris, W. 2010. Properties of dairy-manure-derived biochar pertinent to its
402 potential use in remediation. *Bioresource Technology*, **101**(14), 5222-5228.
403 5. Chen, D., Yu, X., Song, C., Pang, X., Huang, J., Li, Y. 2016. Effect of pyrolysis
404 temperature on the chemical oxidation stability of bamboo biochar. *Bioresource*
405 *Technology*, **218**, 1303-1306.
406 6. Chen, M., Wang, F., Zhang, D.-l., Yi, W.-m., Liu, Y. 2021. Effects of acid
407 modification on the structure and adsorption NH4+-N properties of biochar.
408 *Renewable Energy*, **169**, 1343-1350.
409 7. Cheng, B.-H., Zeng, R.J., Jiang, H. 2017. Recent developments of post-modification
410 of biochar for electrochemical energy storage. *Bioresource Technology*, **246**, 224-233.
411 8. Cross, A., Sohi, S.P. 2013. A method for screening the relative long-term stability of

412 biochar. *Global Change Biology Bioenergy*, **5**(2), 215-220.
413 9. Dong, X., Ma, L.Q., Li, Y. 2011. Characteristics and mechanisms of hexavalent
414 chromium removal by biochar from sugar beet tailing. *Journal of Hazardous*
415 *Materials*, **190**(1), 909-915.
416 10. Feng, D., Zhao, Y., Zhang, Y., Zhang, Z., Che, H., Sun, S. 2017. Experimental
417 comparison of biochar species on in-situ biomass tar H2O reforming over biochar.
418 *International Journal of Hydrogen Energy*, **42**(38), 24035-24046.
419 11. Ghodake, G.S., Shinde, S.K., Kadam, A.A., Saratale, R.G., Saratale, G.D., Kumar,
420 M., Palem, R.R., Al-Shwaiman, H.A., Elgorban, A.M., Syed, A., Kim, D.-Y. 2021.
421 Review on biomass feedstocks, pyrolysis mechanism and physicochemical
422 properties of biochar: State-of-the-art framework to speed up vision of circular
423 bioeconomy. *Journal of Cleaner Production*, **297**, 126645.
424 12. Hadjittofi, L., Prodromou, M., Pashalidis, I. 2014. Activated biochar derived from
425 cactus fibres – Preparation, characterization and application on Cu(II) removal from
426 aqueous solutions. *Bioresource Technology*, **159**, 460-464.
427 13. Han, L., Ro, K.S., Wang, Y., Sun, K., Sun, H., Libra, J.A., Xing, B. 2018. Oxidation
428 resistance of biochars as a function of feedstock and pyrolysis condition. *Science of*
429 *The Total Environment*, **616-617**, 335-344.
430 14. Han, L., Sun, K., Yang, Y., Xia, X., Li, F., Yang, Z., Xing, B. 2020. Biochar's
431 stability and effect on the content, composition and turnover of soil organic carbon.
432 *Geoderma*, **364**, 114184.

15. Harvey, O.R., Kuo, L.-J., Zimmerman, A.R., Louchouarn, P., Amonette, J.E., Herbert, B.E. 2012. An Index-Based Approach to Assessing Recalcitrance and Soil Carbon Sequestration Potential of Engineered Black Carbons (Biochars). *Environmental Science & Technology*, **46**(3), 1415-1421.

16. Huggins, T.M., Pietron, J.J., Wang, H., Ren, Z.J., Biffinger, J.C. 2015. Graphitic biochar as a cathode electrocatalyst support for microbial fuel cells. *Bioresource Technology*, **195**, 147-153.

17. Iriarte-Velasco, U., Sierra, I., Zudaire, L., Ayastuy, J.L. 2016. Preparation of a porous biochar from the acid activation of pork bones. *Food and Bioproducts Processing*, **98**, 341-353.

18. Kazemi Shariat Panahi, H., Dehhaghi, M., Ok, Y.S., Nizami, A.-S., Khoshnevisan, B., Mussatto, S.I., Aghbashlo, M., Tabatabaei, M., Lam, S.S. 2020. A comprehensive review of engineered biochar: Production, characteristics, and environmental applications. *Journal of Cleaner Production*, **270**, 122462.

19. Kim, H.B., Kim, J.G., Kim, T., Alessi, D.S., Baek, K. 2021. Interaction of biochar stability and abiotic aging: Influences of pyrolysis reaction medium and temperature. *Chemical Engineering Journal*, **411**, 128441.

20. Kwak, J.-H., Islam, M.S., Wang, S., Messele, S.A., Naeth, M.A., El-Din, M.G., Chang, S.X. 2019. Biochar properties and lead(II) adsorption capacity depend on feedstock type, pyrolysis temperature, and steam activation. *Chemosphere*, **231**, 393-404.

454 21. Lau, A.Y.T., Tsang, D.C.W., Graham, N.J.D., Ok, Y.S., Yang, X., Li, X.D. 2017.
455 Surface-modified biochar in a bioretention system for Escherichia coli removal from
456 stormwater. *Chemosphere*, **169**, 89-98.
457 22. Lehmann, J. 2007. A handful of carbon. *Nature*, **447**(7141), 143-144.
458 23. Leng, L., Huang, H. 2018. An overview of the effect of pyrolysis process
459 parameters on biochar stability. *Bioresource Technology*, **270**, 627-642.
460 24. Leng, L., Huang, H., Li, H., Li, J., Zhou, W. 2019. Biochar stability assessment
461 methods: A review. *Science of The Total Environment*, **647**, 210-222.
462 25. Leng, L., Li, J., Yuan, X., Li, J., Han, P., Hong, Y., Wei, F., Zhou, W. 2018.
463 Beneficial synergistic effect on bio-oil production from co-liquefaction of sewage
464 sludge and lignocellulosic biomass. *Bioresource Technology*, **251**, 49-56.
465 26. Li, H., Dong, X., da Silva, E.B., de Oliveira, L.M., Chen, Y., Ma, L.Q. 2017.
466 Mechanisms of metal sorption by biochars: Biochar characteristics and modifications.
467 *Chemosphere*, **178**, 466-478.
468 27. Liang, J., Xu, X., Qamar Zaman, W., Hu, X., Zhao, L., Qiu, H., Cao, X. 2019.
469 Different mechanisms between biochar and activated carbon for the persulfate
470 catalytic degradation of sulfamethoxazole: Roles of radicals in solution or solid phase.
471 *Chemical Engineering Journal*, **375**, 121908.
472 28. Liu, C., Wang, W., Wu, R., Liu, Y., Lin, X., Kan, H., Zheng, Y. 2020a. Preparation
473 of Acid- and Alkali-Modified Biochar for Removal of Methylene Blue Pigment. *Acs*
474 *Omega*, **5**(48), 30906-30922.

475 29. Liu, Y., Paskevicius, M., Wang, H., Fushimi, C., Parkinson, G., Li, C.-Z. 2020b.
476 Difference in tar reforming activities between biochar catalysts activated in H2O and
477 CO2. *Fuel*, **271**, 117636.
478 30. Liu, G., Pan, X., Ma, X., Xin, S., Xin, Y. 2020c. Effects of feedstock and inherent
479 mineral components on oxidation resistance of biochars. *Science of The Total*
480 *Environment*, **726**, 138672.
481 31. Liu, Y., Gao, C., Wang, Y., He, L., Lu, H., Yang, S. 2020d. Vermiculite modification
482 increases carbon retention and stability of rice straw biochar at different
483 carbonization temperatures. *Journal of Cleaner Production*, **254**, 120111.
484 32. Lou, K., Rajapaksha, A.U., Ok, Y.S., Chang, S.X. 2016. Pyrolysis temperature and
485 steam activation effects on sorption of phosphate on pine sawdust biochars in
486 aqueous solutions. *Chemical Speciation & Bioavailability*, **28**(1-4), 42-50.
487 33. Manyà, J.J., Ortigosa, M.A., Laguarta, S., Manso, J.A. 2014. Experimental study
488 on the effect of pyrolysis pressure, peak temperature, and particle size on the potential
489 stability of vine shoots-derived biochar. *Fuel*, **133**, 163-172.
490 34. Nan, H., Zhao, L., Yang, F., Liu, Y., Xiao, Z., Cao, X., Qiu, H. 2020. Different
491 alkaline minerals interacted with biomass carbon during pyrolysis: Which one
492 improved biochar carbon sequestration? *Journal of Cleaner Production*, **255**, 120162.
493 35. Nan, H., Yin, J., Yang, F., Luo, Y., Zhao, L., Cao, X. 2021. Pyrolysis temperature-
494 dependent carbon retention and stability of biochar with participation of calcium:
495 Implications to carbon sequestration. *Environmental Pollution*, **287**, 117566.

496 36. Pignatello, J.J., Mitch, W.A., Xu, W. 2017. Activity and Reactivity of Pyrogenic
497 Carbonaceous Matter toward Organic Compounds. *Environ Sci Technol*, **51**(16),
498 8893-8908.
499 37. Sajjadi, B., Chen, W.-Y., Egiebor, N.O. 2019. A comprehensive review on physical
500 activation of biochar for energy and environmental applications. *Reviews in*
501 *Chemical Engineering*, **35**(6), 735-776.
502 38. Shaheen, S.M., Niazi, N.K., Hassan, N.E.E., Bibi, I., Wang, H., Tsang, D.C.W., Ok,
503 Y.S., Bolan, N., Rinklebe, J. 2019. Wood-based biochar for the removal of potentially
504 toxic elements in water and wastewater: a critical review. *International Materials*
505 *Reviews*, **64**(4), 216-247.
506 39. Spokas, K.A. 2010. Review of the stability of biochar in soils: predictability of O:C
507 molar ratios. *Carbon Management*, **1**(2), 289-303.
508 40. Sun, C., Chen, T., Huang, Q., Zhan, M., Li, X., Yan, J. 2020. Activation of
509 persulfate by CO2-activated biochar for improved phenolic pollutant degradation:
510 Performance and mechanism. *Chemical Engineering Journal*, **380**, 122519.
511 41. Wan, Z., Sun, Y., Tsang, D.C.W., Yu, I.K.M., Fan, J., Clark, J.H., Zhou, Y., Cao, X.,
512 Gao, B., Ok, Y.S. 2019. A sustainable biochar catalyst synergized with copper
513 heteroatoms and CO2 for singlet oxygenation and electron transfer routes. *Green*
514 *Chemistry*, **21**(17), 4800-4814.
515 42. Wang, L., O'Connor, D., Rinklebe, J., Ok, Y.S., Tsang, D.C.W., Shen, Z., Hou, D.
516 2020. Biochar Aging: Mechanisms, Physicochemical Changes, Assessment, And

517 Implications for Field Applications. *Environmental Science & Technology*, **54**(23),
518 14797-14814.
519 43. Xiao, X., Chen, B. 2017. A Direct Observation of the Fine Aromatic Clusters and
520 Molecular Structures of Biochars. *Environmental Science & Technology*, **51**(10),
521 5473-5482.
522 44. Xiao, X., Chen, B., Chen, Z., Zhu, L., Schnoor, J.L. 2018. Insight into Multiple and
523 Multilevel Structures of Biochars and Their Potential Environmental Applications: A
524 Critical Review. *Environmental Science & Technology*, **52**(9), 5027-5047.
525 45. Xu, Z., Xu, X., Zhang, Y., Yu, Y., Cao, X. 2020. Pyrolysis-temperature depended
526 electron donating and mediating mechanisms of biochar for Cr(VI) reduction.
527 *Journal of Hazardous Materials*, **388**, 121794.
528 46. Yang, F., Xu, Z., Yu, L., Gao, B., Xu, X., Zhao, L., Cao, X. 2018. Kaolinite
529 Enhances the Stability of the Dissolvable and Undissolvable Fractions of Biochar via
530 Different Mechanisms. *Environmental Science & Technology*, **52**(15), 8321-8329.
531 47. Yang, F., Zhao, L., Gao, B., Xu, X., Cao, X. 2016. The Interfacial Behavior between
532 Biochar and Soil Minerals and Its Effect on Biochar Stability. *Environmental Science*
533 *& Technology*, **50**(5), 2264-2271.
534 48. Yek, P.N.Y., Peng, W., Wong, C.C., Liew, R.K., Ho, Y.L., Wan Mahari, W.A.,
535 Azwar, E., Yuan, T.Q., Tabatabaei, M., Aghbashlo, M., Sonne, C., Lam, S.S. 2020.
536 Engineered biochar via microwave CO2 and steam pyrolysis to treat carcinogenic
537 Congo red dye. *Journal of Hazardous Materials*, **395**, 122636.

538 49. Zhang, M., Song, G., Gelardi, D.L., Huang, L., Khan, E., Mašek, O., Parikh, S.J.,
539 Ok, Y.S. 2020. Evaluating biochar and its modifications for the removal of
540 ammonium, nitrate, and phosphate in water. *Water Research*, **186**, 116303.
541 50. Zhou, Y., Qin, S., Verma, S., Sar, T., Sarsaiya, S., Ravindran, B., Liu, T., Sindhu,
542 R., Patel, A.K., Binod, P., Varjani, S., Rani Singhnia, R., Zhang, Z., Awasthi, M.K.
543 2021. Production and beneficial impact of biochar for environmental application: A
544 comprehensive review. *Bioresource Technology*, 125451.

545 **Table 1.** Basic physicochemical properties of pristine and activated biochars

Biochar	Element content (*wt.*%)				Ash	Yield (%)	H/C[a]	O/C[a]	AI
	C	H	O	N	(*wt.* %)				
BC450	72.2	2.4	23.5	0.3	1.2	32.6	0.40	0.24	0.96
BC550	77.9	2.5	17.2	0.4	1.8	29.0	0.38	0.17	0.96
BC650	87.1	2.1	8.2	0.4	2.1	28.1	0.29	0.07	1.00
BC750	87.9	1.2	8.3	0.2	2.4	25.5	0.17	0.07	1.06
BC850	85.6	0.7	10.4	0.1	3.2	22.5	0.10	0.09	1.10
BC950	88.0	0.7	8.6	0.2	2.5	22.3	0.10	0.07	1.10
BC650-S	71.8	0.8	24.1	0.3	3.0	26.0	0.13	0.25	1.15
BC750-S	83.5	0.6	12.2	0.2	3.5	23.0	0.09	0.11	1.11
BC850-S	86.1	0.4	8.0	0.1	5.5	21.8	0.05	0.07	1.12
BC650-C	74.9	1.0	20.4	0.3	3.4	26.7	0.15	0.20	1.11
BC750-C	83.6	0.8	10.8	0.2	4.6	23.0	0.11	0.10	1.10
BC850-C	90.3	0.4	6.1	0.1	3.1	22.8	0.05	0.05	1.11
BC750-A	82.7	0.6	14.3	0.2	2.2	28.7	0.09	0.13	1.12

[a] Atomic ratio

546

547 **Table 2.** C1s XPS results of pristine and activated biochars

Biochar	C=C(%)	C–O(%)	C=O(%)	COO(%)	Carbonate(%)	O-moiety/ –C=C
BC450	82.3	8.8	2.9	3.1	3.0	0.18
BC550	82.6	7.5	3.6	2.9	3.4	0.17
BC650	82.9	7.5	0.6	4.5	4.6	0.15
BC750	83.8	6.9	2.6	3.0	3.7	0.15
BC850	83.6	6.1	3.7	2.6	4.0	0.15
BC950	84.3	6.6	2.8	2.8	3.5	0.14
BC650-S	81.6	8.1	4.1	1.5	4.6	0.17
BC750-S	82.4	9.4	0.6	4.1	3.4	0.17
BC850-S	82.9	7.4	3.4	2.9	3.4	0.17
BC650-C	82.6	9.8	0.0	3.1	4.5	0.16
BC750-C	81.0	7.6	4.4	2.3	4.7	0.18
BC850-C	82.5	6.2	4.5	2.6	4.2	0.16
BC750-A	84.1	6.4	2.8	3.3	3.4	0.15

548

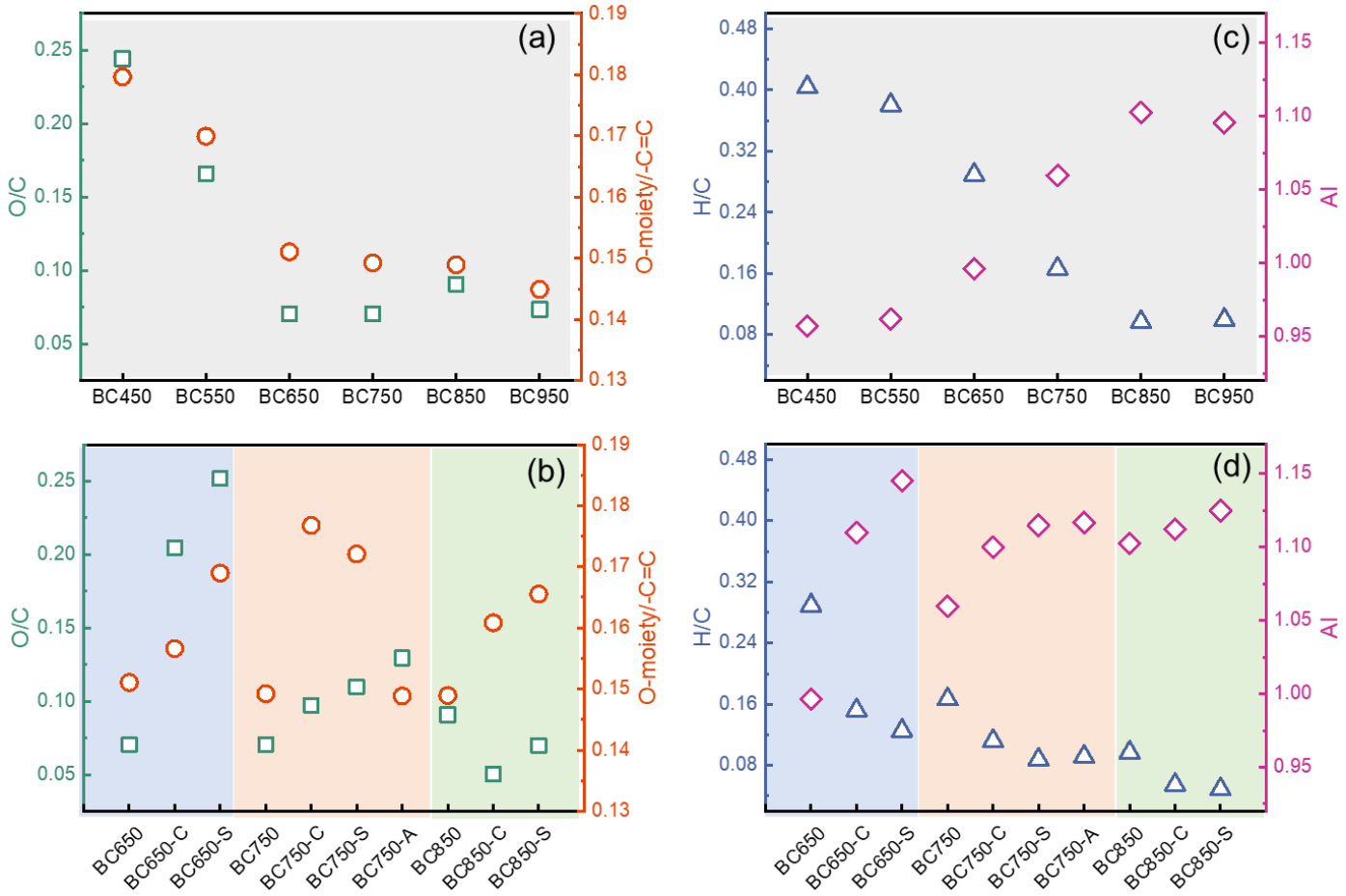

Figure 1. O/C ratio and O-moiety ratio (–C–O + –C=O + –COO/–C=C obtained from XPS analysis) of biochar produced from different pyrolysis temperature (a) and activation methods (b); H/C ratio and Aromatic Index (AI) of biochar produced from different pyrolysis temperature (c) and activation methods (d).

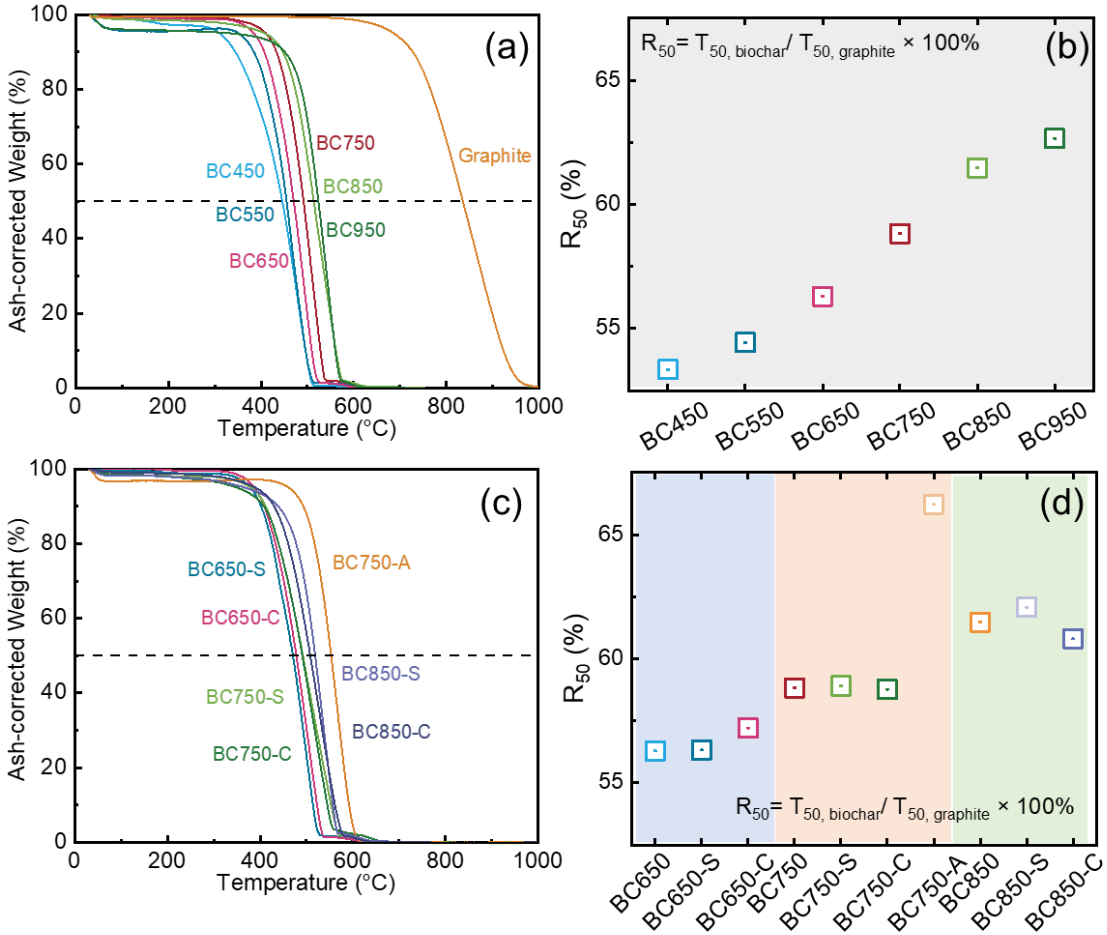

553

554 **Figure 2.** TG analysis of biochar produced from different pyrolysis temperature and activation methods (a, c); Stability of biochar for thermal-
555 oxidation resistance indicated by the TG analysis (R50) (b, d)

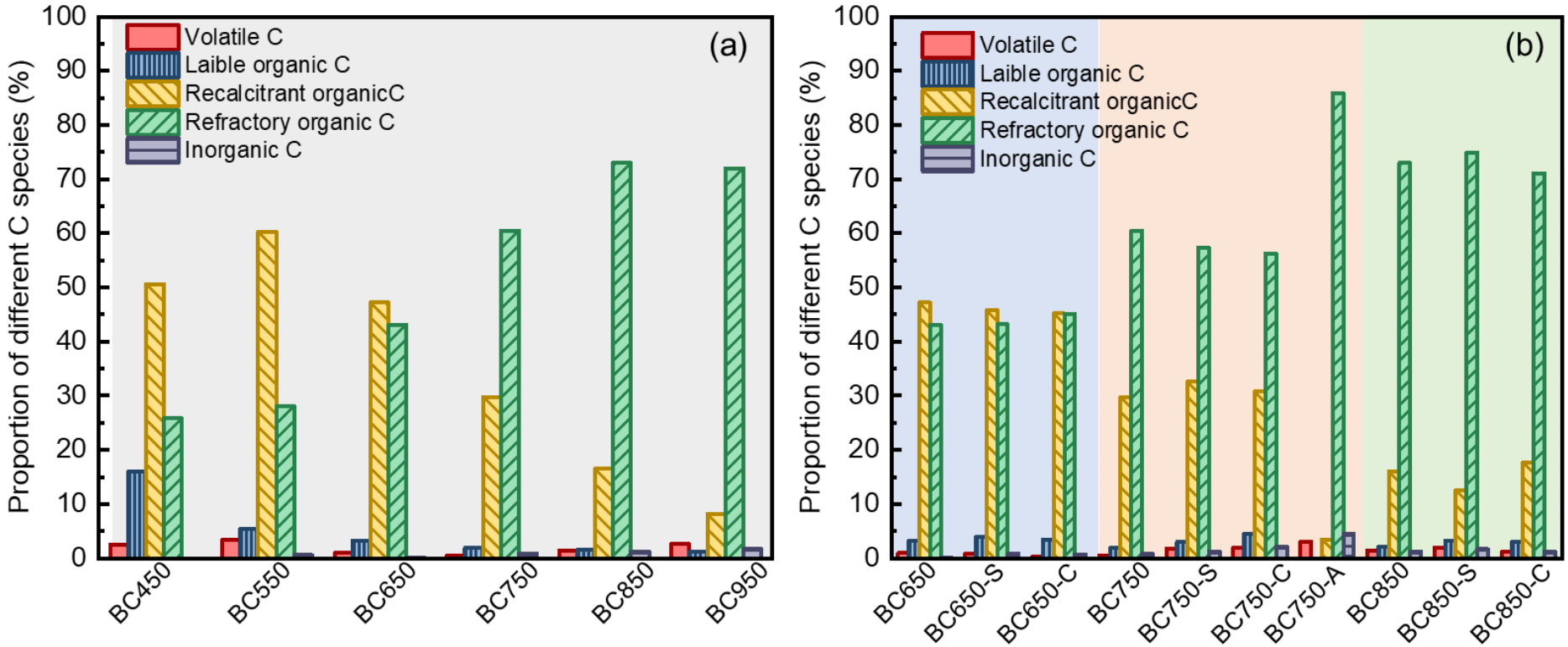

556

557 **Figure 3.** Carbon proportion of biochar produced from different pyrolysis temperature (a) and activation methods (b) obtained by the TG analysis.

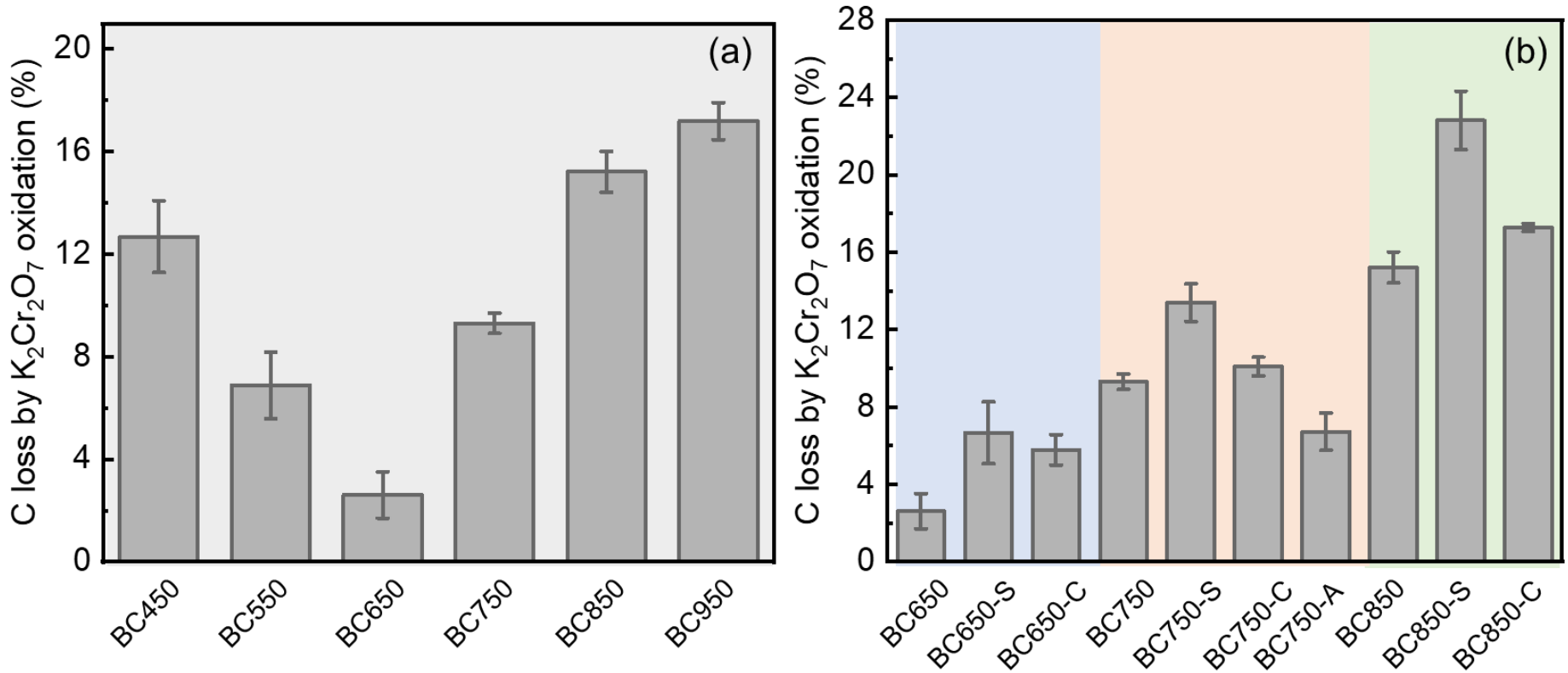

558

559 **Figure 4.** Chemical stability of biochar produced from different pyrolysis temperature (a) and activation methods (b) evaluated by $K_2Cr_2O_7$
560 oxidation methods.

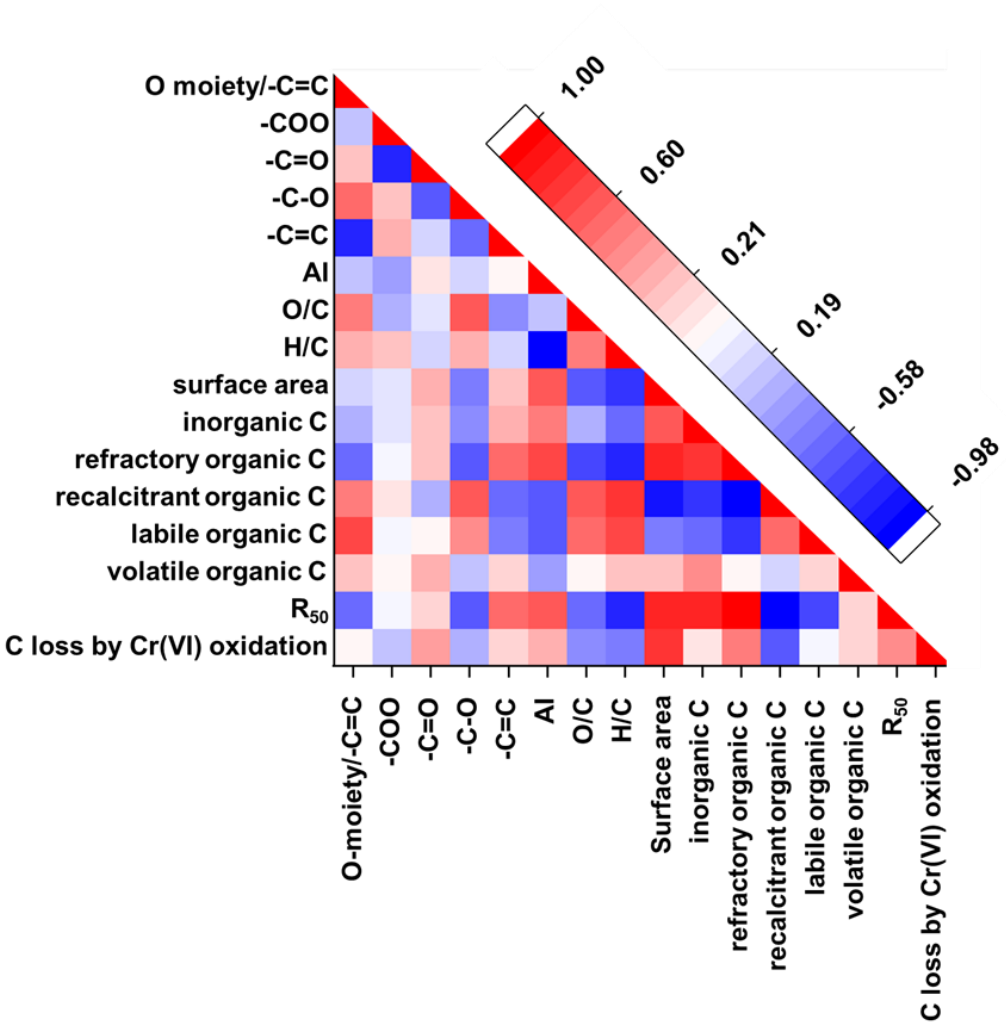

Figure 5. Pearson correlation matrix of the carbon stability indicator and different physiochemical properties of biochars produced from different temperature and activation methods.